8104903

SMITHSONIAN INSTITUTION
ASTROPHYSICAL OBSERVATORY
Cambridge, Mass.

45 p.

Research in Space Science

SPECIAL REPORT

Number 127

(NASA Grant NsG-87-60)

[X] OTS
[X]

ATTITUDE DETERMINATION FROM SPECULAR AND DIFFUSE REFLECTION BY CYLINDRICAL ARTIFICIAL SATELLITES

by

R. H. Giese

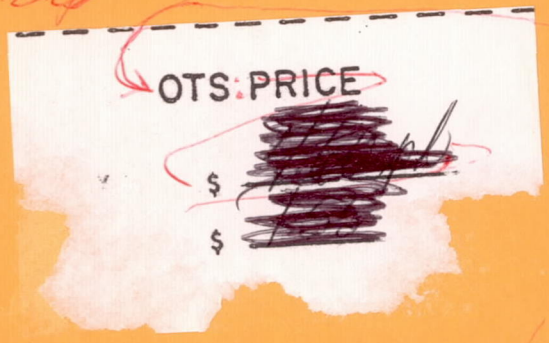

July 8, 1963

5 refs

CAMBRIDGE 38, MASSACHUSETTS

45 p

SAO Special Report No. 127

ATTITUDE DETERMINATION FROM SPECULAR AND DIFFUSE REFLECTION BY CYLINDRICAL ARTIFICIAL SATELLITES

by

R. H. Giese

Smithsonian Institution
Astrophysical Observatory

Cambridge 38, Massachusetts

TABLE OF CONTENTS

ATTITUDE DETERMINATION FROM SPECULAR AND DIFFUSE REFLECTION BY CYLINDRICAL ARTIFICIAL SATELLITES[1, 2]

by

R. H. Giese[3]

Formulae for attitude determination from optical observations are presented for cylindrical artificial satellites with specular reflection. The results allow attitude determination from the observed topocentric coordinates of the reflection flashes and the direction of the sun. Precise knowledge of the orbital data is not needed, and in many cases no expensive optical instruments are necessary to obtain the information on attitude.

For diffuse reflecting cylinders the formula for the intensity as a function of arbitrary angles of illumination and observation is derived and applied to numerical computations of a tumbling cylinder. Author

1. Introduction

The trails of some artificial satellites show a continuous or temporary series of light flashes. These can be attributed to changes in the reflecting conditions due to the satellite's orbital and spinning or tumbling motions. Such flashing outbursts can be used under favorable conditions for attitude determination (Davis, Wells, and Whipple, 1957). An analysis of this type was applied to the carrier rocket of Sputnik III (1958 δ1) by Zessewitch (1958), and Notni and Oleak (1959).

---

[1] Mitteilungen des Astronomischen Instituts der Universität Tübingen No. 66

[2] This work was supported in part by grant NsG 87-60 from the National Aeronautics and Space Administration.

[3] Astronomisches Institut der Universität Tübingen, Germany. Visiting Consultant, Smithsonian Astrophysical Observatory, Cambridge, Mass.

This study of the reflection by cylindrical satellites was made with the purpose of finding new methods or generalizing those mentioned above. The theoretical considerations involve specular cylinders, both circular and polygonal, with and without reflecting ends. The method suggested by Davis, Wells, and Whipple (1957) can be generalized in order to use observations from distant stations and from different passes of the satellite. Baker-Nunn and Moonwatch observations of Tiros I (1960 β2) are discussed in the appendix. The results show that even observations obtained by the inexpensive equipment of a Moonwatch station can be useful for attitude determination of spinning satellites. In the case of tumbling satellites, a method for evaluating photographic exposures (i.e., stationary Baker-Nunn films) and computing the tumbling axis and tumbling period will be discussed.

For diffuse reflecting satellites it is not possible to determine the attitude from the sole fact that reflection is observed at a known angle. A formula for computing the entire light curve of a tumbling cylindrical satellite is presented and illustrated by numerical examples. Similar computations, taking into account the shape and orbital motions of a special satellite, might offer information on tumbling motion when theoretical light curves are compared with photometric observations. Such methods have been applied previously to asteroids, where, however, most observations were made close to opposition and where it was therefore not necessary to consider such general conditions of illumination as are examined here. Section 2 deals with the coordinate systems, their transformations, and the symbols employed in this paper. Section 3 discusses specular reflection and provides the formulae for attitude determination of tumbling and spinning cylinders. In Section 4 we will consider the case of diffuse reflection using Lambert's law.

The formulae derived in this preliminary report will be used in a future discussion of an economical ground-based system for optical attitude determination of satellites carrying no attitude sensors aboard.

2. Basic geometry and definitions

A. Coordinate systems

In the following investigation we shall use three rectangular right-hand coordinate systems:

The equatorial system

The frame of unit vectors $(\vec{c}_1, \vec{c}_2, \vec{c}_3)$ has its origin in the center (i.e., of mass) of the satellite. $\vec{c}_1$ points to the vernal equinox, and $\vec{c}_3$ is parallel to the north direction of the earth's axis.

The rotational system

This frame of unit vectors $(\vec{c}', \vec{c}_2', \vec{c}_3')$ also originates from the center of the satellite, while $\vec{c}_1'$ points towards the ascending node between the plane in which the satellite is spinning or tumbling and the equatorial plane. $\vec{c}_3'$ points in the direction of the angular velocity vector of the spinning or tumbling motion. All symbols referred to in this system will be marked with a prime.

The body system

This frame of unit vectors $(\vec{c}_1'', \vec{c}_2'', \vec{c}_3'')$ is rigidly connected with the satellite. It has its center in the satellite's center. If a tumbling satellite has rotational symmetry, $\vec{c}_3''$ points parallel to the symmetry axis and $\vec{c}_1''$ parallel to the tumbling axis. All symbols referred to in this system will be marked with a double prime.

Figure 1 illustrates the systems for a tumbling cylinder.

B. Direction-angles and unit vectors

To define any direction we either use unit vectors $\vec{u}$ in the above three systems with the components (x,y,z), (x',y',z'), or (x'',y'',z''), respectively, or, alternatively, we give direction-angles (a,δ), (a',δ'), or (a'',δ''), respectively, as shown in figure 2. The transformation equations between direction-vectors and direction-angles are in the equatorial system

$$x = \cos\delta \cos\alpha , \tag{1}$$

$$y = \cos\delta \sin\alpha , \tag{2}$$

$$z = \sin\delta . \tag{3}$$

Analogous transformations are valid in the rotational-plane and body-fixed systems.

In the equatorial system, α denotes the right ascension and δ the declination. For the unit vector $\vec{R}$ in the direction of the rotational axis, we call the components in this system, X,Y,Z, and the direction-angles A (right ascension) and D (declination). Whenever the components of R are obtained, A and D can easily be determined from equations (1) and (3).

C. Relations between the coordinate systems

With the use of the symbols defined above the Eulerian relations yield:

(1) Transformation from equatorial to rotational plane coordinates

$$\begin{pmatrix} x' \\ y' \\ z' \end{pmatrix} = \begin{pmatrix} -\sin A & +\cos A & 0 \\ -\sin D \cos A & -\sin D \sin A & \cos D \\ +\cos D \cos A & +\cos D \sin A & \sin D \end{pmatrix} \begin{pmatrix} x \\ y \\ z \end{pmatrix} . \tag{4}$$

(2) Transformation from the body system to the rotational plane (the angle Φ is defined as in Fig. 1 for a tumbling cylinder)

$$\begin{pmatrix} x' \\ y' \\ z' \end{pmatrix} = \begin{pmatrix} 0 & \sin \Phi & \cos \Phi \\ 0 & -\cos \Phi & \sin \Phi \\ 1 & 0 & 0 \end{pmatrix} \begin{pmatrix} x'' \\ y'' \\ z'' \end{pmatrix} . \tag{5}$$

From equations (1) and (5) we obtain the transformations to be used later:

$$\cos \delta'' \cos \alpha'' = \sin \delta' \tag{6a}$$

$$\cos \delta'' \sin \alpha'' = \cos \delta' \sin (\Phi - \alpha') \tag{6b}$$

$$\sin \delta'' = \cos \delta' \cos (\Phi - \alpha') \tag{6c}$$

$$\tan \alpha'' = \cot \delta' \sin (\Phi - \alpha') . \tag{6d}$$

D. Additional symbols

In addition to the above definitions and symbols, the following will be used throughout this paper:

$\vec{u}_s$, unit vector from satellite to sun;

$\vec{u}_o$, unit vector from satellite to observing station;

$\vec{u}_n$, unit vector normal on a surface element of the satellite (pointing outwards);

$\vec{n}$, normal vector (parallel $\vec{u}_n$, but not a unit vector);

subscript s is added to all components or direction-angles of $\vec{u}_s$,

subscript o is added to all components or direction-angles of $\vec{u}_o$,

subscript n is added to all components or direction-angles of $\vec{u}_n$,

(for example, x_o', y_o', z_o' are components of $\vec{u}_o$ expressed in the rotational plane frame $\vec{c}_1', \vec{c}_2', \vec{c}_3'$);

α_o, 180° + right ascension of the satellite as seen from the observing station;

δ_o, (-1) x declination of the satellite as seen from the observing station;

T, sidereal rotation or tumbling period;

ω, angular velocity;

t, time;

where

$$\omega = \frac{2\pi}{T} . \tag{7}$$

3. Specular reflection

A. The vector normal to the reflecting surface

If any specular reflection is observed, a vector $\vec{n}$ normal to the reflecting surface can be determined by

$$\vec{n} = \vec{u}_s + \vec{u}_o \ . \tag{8}$$

According to the reflection law, $\vec{n}$ is coplanar with $\vec{u}_s$, $\vec{u}_o$, and bisects the angle between $\vec{u}_s$ and $\vec{u}_o$. Thus, in the case of specular reflection, the unit vector normal to the reflecting surface is

$$\vec{u}_n = \frac{\vec{n}}{|\vec{n}|} \ . \tag{9}$$

B. The plane mirror

Plane specular reflecting surfaces of a satellite can be used for attitude determination. For example, one end of a spinning satellite of cylindrical shape is assumed to reflect sunlight toward the observer. In this case, where $\vec{R} = \vec{u}_n$ (fig. 3), the direction of the spin axis unit vector $\vec{R}$ can be found by equation (9):

$$\vec{R} = \begin{pmatrix} X \\ Y \\ Z \end{pmatrix} = \left[(x_s + x_o)^2 + (y_s + y_o)^2 + (z_s + z_o)^2 \right]^{-\frac{1}{2}} \begin{pmatrix} x_s + x_o \\ y_s + y_o \\ z_s + z_o \end{pmatrix} \ . \tag{10}$$

Thus one single observation gives $\vec{R}$ in this simple instance.

C. Tumbling plane mirror

Let us take the example of a black cylinder with one reflecting end assumed to be tumbling about $\vec{R}$ (fig. 4). If at a time t_1 a reflection flash is observed, the normal $\vec{n}_1$ is parallel to the symmetry axis $\vec{c}_3''$ of the cylinder. If at another time t_2 a second flash is observed, the second normal $\vec{n}_2$ is parallel to the orientation of $\vec{c}_3''$ at t_2.

Since $\vec{c}_3''$ is always perpendicular to $\vec{R}$ (tumbling condition), we obtain a vector $\vec{r}$ parallel to the unit vector $\vec{R}$ by

$$\vec{r} = \vec{n}_1 \times \vec{n}_2 \, . \tag{11}$$

If the known direction vectors at the times t_1 and t_2 are $\vec{u}_{01}$, $\vec{u}_s$ and $\vec{u}_{02}$, $\vec{u}_{s2} = \vec{u}_s + \Delta\vec{u}_s$, respectively, we obtain

$$\vec{r} = \begin{vmatrix} \vec{c}_1 & \vec{c}_2 & \vec{c}_3 \\ x_{01} + x_s & y_{01} + y_s & z_{01} + z_s \\ x_{02} + x_s + \Delta x_s & y_{02} + y_s + \Delta y_s & z_{02} + z_s + \Delta z_s \end{vmatrix} , \tag{12}$$

or

$$\vec{r} = D_1\vec{c}_1 + D_2\vec{c}_2 + D_3\vec{c}_3 \, , \tag{13}$$

with

$$D_1 = \begin{vmatrix} +1 & y_s & z_s \\ -1 & y_{01} & z_{01} \\ -1 & y_{02} + \Delta y_s & z_{01} + \Delta z_s \end{vmatrix} , \tag{14}$$

$$D_2 = \begin{vmatrix} -1 & x_s & z_s \\ +1 & x_{01} & z_{01} \\ +1 & x_{02} + \Delta x_s & z_{02} + \Delta z_s \end{vmatrix} , \qquad (15)$$

$$D_3 = \begin{vmatrix} +1 & x_s & y_s \\ -1 & x_{01} & y_{01} \\ -1 & x_{02} + \Delta x_s & y_{02} + \Delta y_s \end{vmatrix} . \qquad (16)$$

Finally, we obtain the unit vector in the direction of the tumbling axis

$$\vec{R} = \left[D_1^2 + D_2^2 + D_3^2 \right]^{-\frac{1}{2}} \cdot \begin{pmatrix} D_1 \\ D_2 \\ D_3 \end{pmatrix} . \qquad (17)$$

In this case two observations are necessary to determine $\vec{R}$.

D. Spinning cylinder

Let us assume a cylinder with black ends, but with reflecting sides. In the case of the body system, equation (8) can be written as

$$\vec{n} = (\cos \delta_s'' \cos \alpha_s'' + \cos \delta_o'' \cos \alpha_o'') \vec{c}_1''$$
$$+ (\cos \delta_s'' \sin \alpha_s'' + \cos \delta_o'' \sin \alpha_o'') \vec{c}_2'' + (\sin \delta_s'' + \delta_o'') \vec{c}_3'' . \qquad (18)$$

Since $\vec{n}$ is perpendicular to $\vec{c}_3''$ (see fig. 6),

$$\sin \delta_s'' + \sin \delta_o'' = 0 . \qquad (19)$$

Hence, given a direction-angle δ''_s of the sun, we can observe reflection at the direction-angle $\delta''_o = -\delta''_s$. From equation (18) we can find the position of the reflecting line on the cylinder side (fig. 6), and we have

$$\tan \alpha''_n = \frac{\sin \alpha''_s + \sin \alpha''_o}{\cos \alpha''_s + \cos \alpha''_o} . \tag{20}$$

Equation (20) involves no limitation in this case, since the entire surface of the side of the cylinder is assumed to be specular. Thus, equation (19) remains the sole condition for observing a reflection.

In the case of the wholly reflecting cylinder, reflection will be observed on a complete cone. The axis of the cone is the cylinder axis, and the opening angle is $90^\circ - \delta_s$. The intersection (see fig. 7) of this light cone with the earth's surface may be called the "flash line," since everywhere along this line a reflection-flash will be seen. Depending on the direction of the orbital motion of the satellite, this flash line will encounter an observation station once or twice during one pass. Since equation (19) states that normal vectors $\vec{n}$ derived from observed flashes must be perpendicular to $\vec{c}'''_3$, and thus perpendicular to the spin axis, we obtain from the normal vectors $\vec{n}_1$ and $\vec{n}_2$ (corresponding to the observation times t_1 and t_2) the vector $\vec{r}$ (equation (11)) and

$$\vec{R} = \frac{\vec{n}_1 \times \vec{n}_2}{|\vec{n}_1 \times \vec{n}_2|} . \tag{21}$$

A method for obtaining $\vec{R}$ from the observations of two neighboring stations during the same pass has been presented by Davis, Wells, and Whipple (1957). Their solution is contained in (17) as a special case for $\Delta x_s = \Delta y_s = \Delta z_s = 0$. The general solution (17), however, includes the determination of $\vec{R}$ from different passes, even if considerably apart in time and from the same or from different and distant stations, as long as $\vec{R}$ does not noticeably change its direction between the observations.

While in principle $\vec{R}$ can be obtained by two observations, it should be noted that the method described above fails if the normal vectors $\vec{n}_1$ and $\vec{n}_2$ used in equation (11) have approximately the same direction. Since these normal vectors as computed from the observations are affected by the error vectors $\delta\vec{n}_1$, $\delta\vec{n}_2$, respectively, we obtain instead of $\vec{r}$ (eq. 11) a vector $(\vec{n}_1 + \delta\vec{n}_1) \times (\vec{n}_2 + \delta\vec{n}_2)$ which is different from $\vec{r}$ by

$$\delta\vec{r} = \delta\vec{n}_1 \times \vec{n}_2 + \vec{n}_1 \times \delta\vec{n}_2 \ . \tag{22}$$

This vector is approximately equal to $\vec{r}$ only if $|\vec{r}| \gg |\delta\vec{r}|$, which is not the case if $\vec{n}_1$ is approximately parallel or antiparallel to $\vec{n}_2$.

If more than two observations are available, the vector $\vec{R}$ might be found by minimizing the sum

$$[vv] = \sum_{i=1}^{z} (\vec{u}_{ni} \cdot \vec{R})^2 \ . \tag{23}$$

If both R and all z normal vectors $\vec{u}_{ni}$ obtained from equation (9) are correct, $[vv]$ equals zero, since $(\vec{u}_{ni}\vec{R}) = \cos 90^\circ$. The correct vector $\vec{R}$ can be found by systematic iterative trials, choosing appropriate pairs of direction angles A,D. Since, however, the vectors $\vec{u}_{ni}$ obtained by the observations are affected by errors, the best pair A,D will hardly result in $[vv] = 0$, but will rather result in a minimum value of $[vv]$.

While so far the problems discussed here, that of the tumbling mirror, and even that of a spinning black cylinder with M discrete mirrors or reflecting sides (fig. 5), result in the same equation (17), there remains a marked difference in the effect described in equation (20). Although, as indicated above, equation (20) is ineffective in the case of the wholly reflecting cylinder, it strongly affects reflection in the case of a cylinder such as that in figure 5. Even if the condition (19) is fulfilled in the case of figure 5, a reflection will be observed only if one of the mirrors happens to be at the position satisfying equation (20). Thus, in the case of the cylinder in figure 5, reflection will be observed only in the direction of M discrete rays each forming an angle $(-\delta''_s)$ with the body system.

If the sun were a point source of light, at a certain observing station only an "infinite short" reflection flash would be visible in the case of a spinning cylinder with reflecting sides, if equation (19) is satisfied. Since, however, the sun is not a point source, the reflection flash will last a finite time and thus cover a part of the finite length of the satellite's trail. If the side of the satellite is covered with discrete mirrors (fig. 5), or if the satellite is polygonal, this single flash will disintegrate into several shorter flashes due to the spinning rotation, since here equation (20) must also be satisfied.

Tiros satellites are examples where the formulae for a spinning cylinder may be applied. All eighteen sides, as well as the top of these polygonal cylinders have plane surfaces. They therefore meet the conditions of the models studied above. It should be noted, however, that since the bottom of the Tiros is a rather complicated supporting structure, some difficulties might arise if reflection from the bottom of the satellite is observed. Figure 8 illustrates the shape of Tiros II (1960 π2), and shows side surfaces and the base. Baker-Nunn films, made from Tiros I (1960 β2), the structure of which is identical with Tiros II, show general features that fit the theory. Figure 9a shows an outburst of flashes. The single flashes might be attributed to the side surfaces. The increase and decrease in intensity are due to the fact that equation (19) is fulfilled only for a finite portion of the trail. Figures 9a and 9b verify that just fifteen seconds after an outburst of specular flashes (9b) a trail of steady intensity, presumably due to diffuse reflection, is visible (9c).

In the case of a spinning cylinder with M reflecting surfaces (fig. 5), the rotational period T can be approximately determined from the time difference $(t_2 - t_1)$ between two consecutive flashes as $T \approx (t_2 - t_1).M.$ The satellite, however, moves along its orbit during this interval of time, hence the exact sidereal period of rotation is

$$T = \frac{t_2 - t_1}{1/M + \frac{\Delta\Phi}{2\pi}} . \tag{24}$$

From the normal vectors $\vec{u}_{n1}$ and $\vec{u}_{n2}$, corresponding to t_1 and t_2, the angle $\Delta\Phi$ can be determined from

$$|\sin \Delta\Phi| = |\vec{u}_{n1} \times \vec{u}_{n2}| , \tag{25}$$

and

$$\cos \Delta\Phi = (\vec{u}_{n1} \cdot \vec{u}_{n2}) . \tag{26}$$

If the direction of rotation is known, the remaining ambiguity of the solution between $\Delta\Phi$ and $-\Delta\Phi$ can be solved.

E. Tumbling cylinder

If the cylinder, instead of spinning about $\vec{c}_3''$, tumbles about $\vec{c}_1''$, we obtain the transformation of the reflecting condition (19) into the rotational-plane system by means of equation (6c). In this way we find the rotational angle Φ_f if a reflection flash is observed from the direction vectors $\vec{u}_s$ and $\vec{u}_o$:

$$\cot \Phi_f = - \frac{\cos \delta_s' \sin \alpha_s' + \cos \delta_o' \sin \alpha_o'}{\cos \delta_s' \cos \alpha_s' + \cos \delta_o' \cos \alpha_o'} , \tag{27a}$$

$$\cot \Phi_f = - \frac{y_s' + y_o'}{x_s' + x_o'} . \tag{27b}$$

From transformation (4), we obtain in the equatorial system:

$$\cot \Phi_f = \frac{\sin D \cos A \, (x_s + x_o) + \sin D \sin A \, (y_s + y_o) - \cos D \, (z_s + z_o)}{\cos A \, (y_s + y_o) - \sin A \, (x_s + x_o)} . \tag{27c}$$

Equation (27c) is identical with the condition expressed in direction angles α_n, δ_n of the normal to the cylinder surface $\vec{u}_n$, as found by Zessewitch (1958):

$$\cot \Phi_f = - \tan \delta_n \cdot \frac{\cos D}{\sin(\alpha_n - A)} + \sin D \cot (\alpha_n - A) . \tag{27d}$$

To find A and D, Notni and Oleak (1959) developed and successfully applied a partially graphic method to the carrier rocket (1958 β1) of Sputnik III. Another method appropriate for electronic computation is proposed as follows:

In equation (27c) the numerator and denominator of the right side are functions $f(A,D,\vec{u}_s,\vec{u}_o)$ and $g(A,\vec{u}_s,\vec{u}_o)$, respectively, of the unknown direction-angles A,D, and of the components of the direction-vectors $\vec{u}_s,\vec{u}_o$, as observed at the time t of observation. We will assume that the the $\vec{u}_s,\vec{u}_o$ are correct. The angles A,D might be completely unknown. The tumbling period as observed only approximates the true sidereal tumbling period T, since the satellite changes its position during the time between two reflection flashes. If during one pass z flashes are observed in the satellite trail, we obtain from the first flash $\Phi_f = \Phi_1$ and

$$f_1 = f(A,D,\vec{u}_{s1},\vec{u}_{o1}) \ , \quad g_1 = g(A,\vec{u}_{s1},\vec{u}_{o1}) \ ,$$

hence

$$\cot \Phi_1 = \frac{f_1}{g_1} \ , \tag{28}$$

and from the following flashes at the times t_i $(i = 2,3,\ldots z)$, using Φ_1 as found from (28),

$$\Delta_i = g_i \cos\left(\Phi_1 + 2\pi \frac{t_i - t_1}{T}\right) - f_i \sin\left(\Phi_1 + 2\pi \frac{t_i - t_1}{T}\right) . \tag{29}$$

Δ_i would be zero if we substituted the correct values of T,A,D. Since we do not know these, we try to minimize the sum:

$$[vv] = \sum_{i=2}^{z} (\Delta_i)^2 \ . \tag{30}$$

For this we start with T equal to the observed, approximate tumbling period, and determine by systematic trials the pair A,D that minimizes $[vv]$. With such a pair T will be improved, and then A,D, and so on. As long as A,D are to be determined within an accuracy of some degrees, the inaccuracy of about 1/3 minute of arc of the measured positions of the flashes might be neglected. Thus, the use of only the first flash for determining Φ_1 is not a severe restriction.

An example of a tumbling cylinder is the carrier rocket of Echo I (1960 ι2), which tumbled after separation from Echo. Figure 10 shows the cylindrical side surface of the rocket and, in particular, the flashing stripe due to specular reflection of the illuminating devices. Baker-Nunn exposures of the flashes, due to the tumbling of this satellite, appear in figures 9d and 9e.

4. Diffuse reflection

A. Lambert's law

If ρ is the reflectivity ($0 \leq \rho \leq 1$) and $F\left[\frac{\text{energy}}{\text{area} \cdot \text{time}}\right]$ is the incoming solar flux of light, the intensity $dJ\left[\frac{\text{energy}}{\text{solid angle} \cdot \text{time}}\right]$ reflected by a surface element dA of the diffuse reflecting area, is given by Lambert's law as

$$dJ = \frac{F \cdot \rho}{\pi} \cdot (\vec{u}_s \vec{u}_n)\,(\vec{u}_o \vec{u}_n)\,dA \,. \tag{31}$$

The scalar products $(\vec{u}_s \vec{u}_n)$ and $(\vec{u}_o \vec{u}_n)$ give the cosines of the angles between the incident light and the normal vector $\vec{u}_n$, and between the light reflected in the direction towards the observer and $\vec{u}_n$. These angles are not necessarily equal, as in Section 3. In the case of diffuse reflection, the condition for observing reflected light is

$$(\vec{u}_s \vec{u}_n) > 0 \quad \text{and} \quad (\vec{u}_o \vec{u}_n) > 0 \,. \tag{32}$$

Otherwise, J = 0, since the surface is either not illuminated or is not visible to the observer, whether illuminated or not.

B. Plane end of a tumbling cylinder

For a plane end of a tumbling cylinder (fig. 4) we obtain from equation (31), after transformation into the rotational plane system (eq. 6c),

$$J = \frac{F\rho A}{\pi}\left[\cos\,\delta_s'\cos\,(\Phi - \alpha_s')\right]\left[\cos\,\delta_o'\cos\,(\Phi - \alpha_o')\right] \tag{33}$$

if both brackets > 0. Otherwise, J = 0.

Equation (33) can be written as

$$J = \frac{F\rho A}{\pi}\left[x_s' \cos\Phi + y_s' \sin\Phi\right]\left[x_o' \cos\Phi + y_o' \sin\Phi\right] , \qquad (34)$$

and, if necessary, can be transformed by equation (4) into the equatorial system. If both ends are taken into account, the equation is valid, but only the product of the two brackets in (33) is required to be > 0 in order to obtain an intensity $J > 0$.

C. Side of a tumbling cylinder

If we consider the diffuse reflection by the side of a cylinder of length ℓ and diameter d, we obtain from equation (31) in the body-fixed system by a stripe

$$dA = \frac{\ell d}{2}\, d\alpha_n'' \qquad (35)$$

on the cylinder surface (fig. 6). The intensity contribution

$$dJ = \frac{F\rho}{\pi}\left[x_s'' x_n'' + y_s'' y_n''\right]\left[x_o'' x_n'' + y_o'' x_n''\right] dA , \qquad (36)$$

since the component of $\vec{u}_n$ in the direction of $\vec{c}_3''$ is $z_n'' = 0$. Transformation into direction-angles (eq. 1) yields, after application of trigonometric addition formulae and substitution of (35),

$$dJ = \frac{F\rho\ell d}{4\pi} \cos\delta_s'' \left[\cos(\alpha_s'' - \alpha_o'') + \cos(\alpha_s'' + \alpha_o'' - 2\alpha_n'')\right] d\alpha_n . \qquad (37)$$

The surface visible to the observer and illuminated at the same time lies between the limits $\alpha_s'' - \frac{\pi}{2} \le \alpha_n'' \le \alpha_o'' + \frac{\pi}{2}$, if $\alpha_s'' > \alpha_o''$, and between $\alpha_o'' - \frac{\pi}{2} \le \alpha_n'' \le \alpha_s'' + \frac{\pi}{2}$, if $\alpha_s'' < \alpha_o''$. Using these limits of α_n'' to integrate equation (37), we obtain

$$J = \frac{F\rho\ell d}{4\pi} \cos\delta_o'' \cos\delta_s'' \left[(\pi - |\vartheta''|)\cos\vartheta'' + |\sin\vartheta''|\right] \qquad (38)$$

with

$$\vartheta'' = \alpha''_s - \alpha''_o \ . \tag{39}$$

Equation (38) is valid for both $\alpha''_s \geq \alpha''_o$ and $\alpha''_s < \alpha''_o$. It includes, as a special case ($\delta''_s = \delta''_o = 0, \vartheta'' > 0$), the result found by Laughlin and Bauer (1961). The variation of the intensity with ϑ'' is shown in figure 11.

If we consider a tumbling cylinder, we must transform equations (38) and (39) by means of equations (6). This yields

$$\cos \vartheta'' = \frac{B}{\cos \delta''_s \cos \delta''_o} \ , \tag{40a}$$

$$\sin \vartheta'' = \frac{A}{\cos \delta''_s \cos \delta''_o} \ , \tag{40b}$$

$$\tan \vartheta'' = \frac{A}{B} \ , \tag{40c}$$

with

$$A = \cos \delta'_s \sin \delta'_o \sin (\Phi - \alpha'_s) - \sin \delta'_s \cos \delta'_o \sin (\Phi - \alpha'_o) \ , \tag{41a}$$

$$B = \sin \delta'_s \sin \delta'_o - \cos \delta'_s \cos \delta'_o \sin (\Phi - \alpha'_s) \sin (\Phi - \alpha'_o) \ . \tag{41b}$$

Finally,

$$J = \frac{F \rho \ell d}{4\pi} \left[(\pi - \text{function } \frac{A}{B}) \cdot B + |A| \right] , \tag{41c}$$

with

$$\text{function } \frac{A}{B} = \begin{cases} |\arctan \frac{A}{B}| & \text{if } B > 0 \\ \frac{\pi}{2} & \text{if } B = 0 \\ \pi - |\arctan \frac{A}{B}| & \text{if } B < 0 \ . \end{cases} \tag{41d}$$

To get an idea of the intensity variations caused by tumbling, some numerical examples were computed by means of equations (41). The results appear in the rotational system. To remain independent of the special direction of c_1' and to achieve some symmetry in the curves, all results are expressed as a function of the angles ψ and α' (fig. 12):

$$\psi = \Phi - \frac{\alpha_s' + \alpha_o'}{2} , \tag{42}$$

$$\alpha' = \frac{\alpha_s' - \alpha_o'}{2} . \tag{43}$$

Results for a cylinder with black ends and diffuse reflecting sides are given in figures 12 through 15. In figure 13 the sun's direction is assumed to be above and perpendicular to the tumbling plane ($\delta_s' = 90^\circ$).

If the observer looks from this direction he sees no variations. If he is situated in the rotational plane ($\delta_c' = 0$), he sees marked variations - no intensity if the black end points towards him, but maximum intensity if he views the cylinder from the side. From underneath the tumbling plane ($\delta_o' < 0$), the closer δ_o' approaches -90° the less does the observer see the illuminated portion of the cylinder surface, and when $\delta_o' = -90^\circ$, only the dark side of the cylinder is visible.

Some of the features outlined above occur again in the more general cases illustrated in figures 14 through 16. In figure 14 both the sun ($\delta_s' = 30^\circ$) and the observer ($\delta_o' = 15^\circ$) are above the tumbling plane and thus the intensity never drops to zero. On the other hand, if the observer is looking from underneath the tumbling plane ($\delta_o' = -45^\circ$), as in figure 15, the intensity observed is in general rather low, even at its maximum. In figure 16, the sun and the observer are in the tumbling plane. The intensity observed is zero from all positions $\psi < \alpha'$ and $\psi > \pi - \alpha'$, since in these cases only the shadow side of the cylinder is seen. It should be emphasized that the positions of the maxima of intensity do not in general agree with the angles ψ_f obtained from the angles Φ_f which would give a reflection flash in the specular case. These flash positions are marked by large dots in figures 13 through 16. If the cylinder has diffuse reflecting ends, the observable intensity can be computed from equations (33) and (41c). Examples are presented in figures 16 through 21, where in all cases the product of the length and the diameter of the cylinder is assumed to be a constant. If we compare results for a long cylinder ($\frac{d}{\ell} = \frac{1}{6}$) (figs. 17,20) and for a short and thick cylinder ($\frac{d}{\ell} = \frac{1}{2}$) (figs. 18, 21) with the curves for a cylinder with black ends (figs. 16, 19), at the same angles of illumination and observation, we find the greatest deviations for $\frac{d}{\ell} = \frac{1}{2}$, due to the large surface of the diffuse reflective ends.

The breaks in the curve, particularly noticeable in figures 17, 18, and 21, are seen at those positions where either the ends or the side become visible (or invisible) to the observer.

Appendix

Spinning satellite with specular reflection: Tiros I (1960 β2).

To obtain an idea of the practical applicability of the methods described above, observations by Moonwatch and Baker-Nunn stations were searched for reports of flashing outbursts. More complete Moonwatch data including definite observations of flashing phenomena of Tiros I, available for July 1960, are presented in table 1. Another set of observations by Baker-Nunn stations is presented in table 2. It should be noted, however, that these films were not exposed for the purpose of obtaining information on the spinning motion of Tiros. They merely represent examples recording occasional flashing phenomena on an orientation frame or on a time exposure. Thus, unfortunately, in all exposures only a portion of the outbursts appear. The positions in table 2 correspond to the beginning (B), middle (M), or end (E) of the recorded trail, depending on where the brightest flashes were seen.

The data presented in table 2 were used to compute $\vec{u}_o$ and the normal vector $\vec{u}_n$ on the reflecting surface (α_n, δ_n). Since the position of the spin axis was approximately known (Bandeen and Manger, 1960), the angle $\vec{R}\,\vec{u}_n$ between $\vec{u}_n$ and the spin axis could be computed. The results show that this angle was close to 90°. Thus, reflection from the sides of Tiros can be assumed. Only the observations of May 5 and 6 result in angles close to 0°, which suggests that the reflections might come from the ends of the cylinder. The average deviation from 90° (or 0°) is about ± 7°. This is not surprising in view of the difficulties of determining the center of the flash outbursts outlined above and the uncertainty in the direction of $\vec{R}$ in the diagram of Bandeen and Manger.

Acknowledgments

I wish to thank Professor H. Siedentopf of the University of Tübingen for granting me leave-of-absence for two and a half months to carry out this study in Cambridge. Professor F. L. Whipple made this possible by providing travel expenses and allowing me to take advantage of the facilities of the Smithsonian Astrophysical Observatory. I am deeply grateful to him and to Dr. G. Colombo, Mr. I. G. Izsak, and Dr. C. Lundquist for valuable discussions. Lastly, I owe special gratitude to all members of the staff who helped to find and process the observational data referred to in this paper.

References

BANDEEN, W. R. and MANGER, W. P.

1960. Angular motion of the spin axis of the Tiros I Meteorological Satellite due to magnetic and gravitational torques. Journ. Geophys. Res. 69, 9, p. 2992.

DAVIS, R. J., WELLS, R. C., and WHIPPLE, F. L.

1957. On determining the orientation of a cylindrical artificial earth-satellite. Astronautica Acta 3, p. 231.

LAUGHLIN, R. D. and BAUER, G. A.

1961. Specular and diffuse reflection from spheres and cylinders. Communication from Pennsylvania State University, State College, Pa.

NOTNI, P. and OLEAK, H.

1959. Die Rotation der Trägerrakete von Sputnik III (1958 δ1). Veröffentlichungen der Sternwarte Babelsberg, vol. 13, p. 4.

ZESSEWITCH, W. P.

1958. Über den Lichtwechsel der Sowjetischen Künstlichen Erdsatelliten. IAU Meeting, Moscow.

TABLE 1

Moonwatch Observations of definite Flashing outbursts of Tiros I

Observation No.	DATE	UT	SITE NO.	STATION	$-\alpha_o$	$-\delta_o$	α_n	δ_n	A	D	$\sphericalangle \vec{R}\,\vec{u}_n$
1	1960 July 3	$02^h36^m52^s$	8571	Pittsburgh	16^h03^m	21°48'	+ 81°	1°	165°	0°	84
2	July 4	03 25 13	0140	St.Louis	13 57.7	52 20	+ 74	-17	165	0	90
3	July 11	04 11 19	8536	N. Canton	18 56	85 33	+290	-31	168	+20	76
4	July 13	02 24 39	8565	N. Canton	00 59	83 09	+299	-33	171	+28	78
5	July 15	02 21 58	8559	N. Canton	22 35	86 47	+297	-33	173	+30	106
6	July 15	02 22 14	8554	N. Canton	21 33.7	80 15	+299	-30	173	+30	79
7	July 15	02 22 15	8565	N. Canton	21 53	79 15	+300	-29	173	+30	78
8	July 15	04 05 32	8565	N. Canton	15 30	42 03	+ 87	-12	173	+30	92
9	July 17	04 02 40	8565	N. Canton	15 07	14 06	+ 80	+ 4	178	+36	93
10	July 18	03 09 08	0140	St.Louis	19 17	63 02	+295	-21	178	+36	83
11	July 18	03 10 29	8565	N. Canton	19 49.5	24 32	+275	- 2	178	+36	85
12	July 20	04 44 36	8517	Sacramento	18 10	52 39	+289	-16	184	+39	89
13	July 21	02 14 48	8564	Rochester	15 12	00 45	+ 82	+13	189	+40	94
14	July 21	05 35 18	8517	Sacramento	17 34.4	06 24	+281	+ 7	189	+40	83

TABLE 2

Baker-Nunn Films showing Flashing outbursts of Tiros I

Observation No.	DATE	UT	FILM NO.	STATION	$-\alpha_o$	$-\delta_o$	α_n	δ_n	A	D	$\sphericalangle \vec{R}\,\vec{u}_n$	Reference Position
15	1960 May 5	$09^h39^m47^s$	11-1005	Villa Dolores(Arg.)	$21^h23.9^m$	+21°33'	271	- 4	90°	+ 2°	6	M
16	May 6	08 44 07	7-1529	Arequipa (Peru)	22 18.8	+ 2 34	281	+12	90	+ 2	15	B
17	May 6	08 47 36	11-1014	Villa Dol. (arg.)	22 28.8	+20 19	270	- 3	90	+ 2	11	M
18	May 26	01 11 41	10-1340	Jupiter (Florida)	09 18	-30 41	14	+38	145	+35	94	M
19	May 27	00 23 35	9-1364	Curacao (NWI)	10 34.2	-32 10	23	+34	145	+35	91	E
20	June 2	23 29 03	7-1687	Arequipa (Peru)	12 31.2	-57 47	49	+44	158	+12	95	M
21	June 4	23 25 48	7-1701	Arequipa (Peru)	7 23	-60 14	43	+63	158	+ 8	93	M
22	June 4	23 27 02	7-1701	Arequipa (Peru)	8 10	-79 08	63	+59	158	+ 8	86	M
23	July 20	04 47 49	1-2252	Organ Pass (N.M.)	16 14.2	+45 08	276	-14	184	+39	97	B
24	July 20	04 47 27	1-2252	Organ Pass (N.M.)	15 15.8	+49 26	271	-17	184	+39	103	M
25	July 24	01 22 12	10-1602	Jupiter (Florida)	20 20.5	+31 21.8	304	- 6	202	+38	84	M

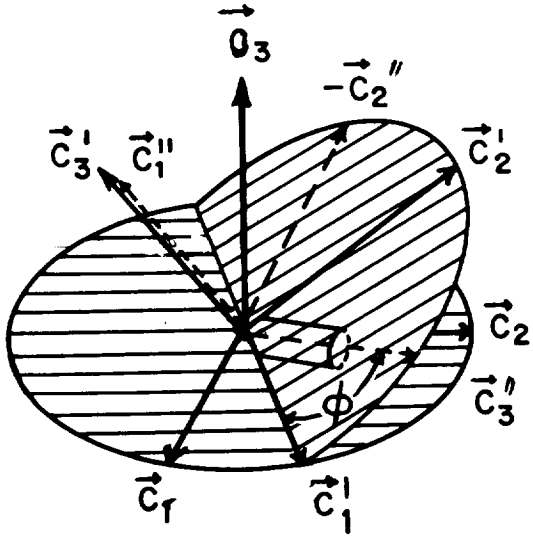

Figure 1.--Geometry of the coordinate Systems

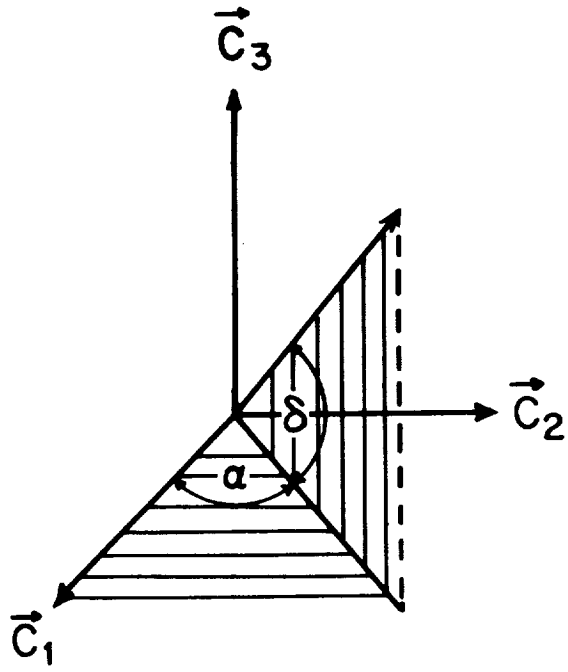

Figure 2.--Definition of the direction angles

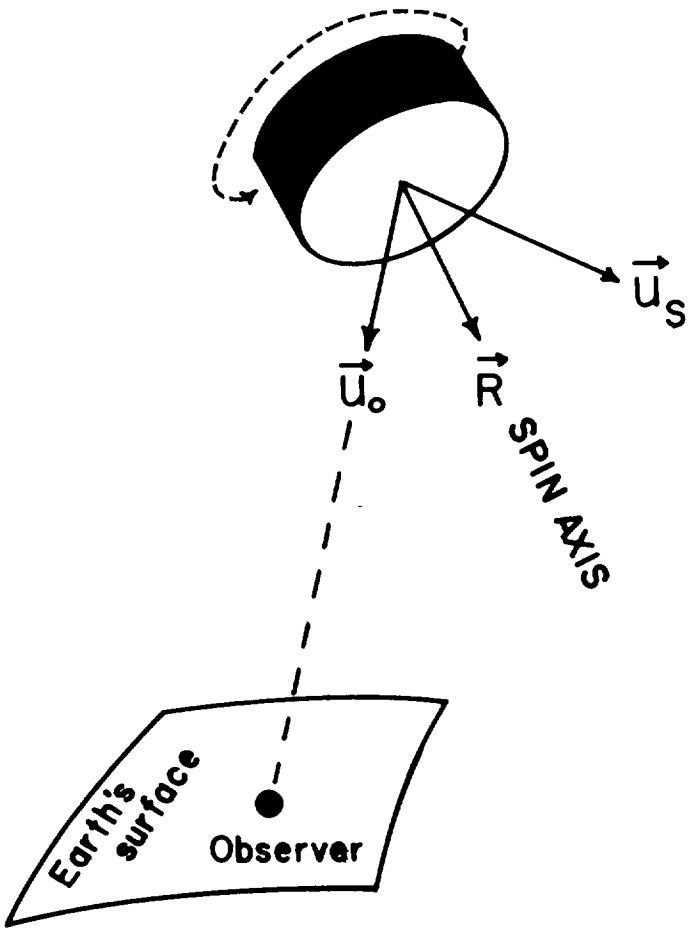

Figure 3.--Spinning Satellite with reflecting plane end: $\vec{u}_s$, direction towards sun; $\vec{u}_o$, direction towards observer; $\vec{R}$, spin axis

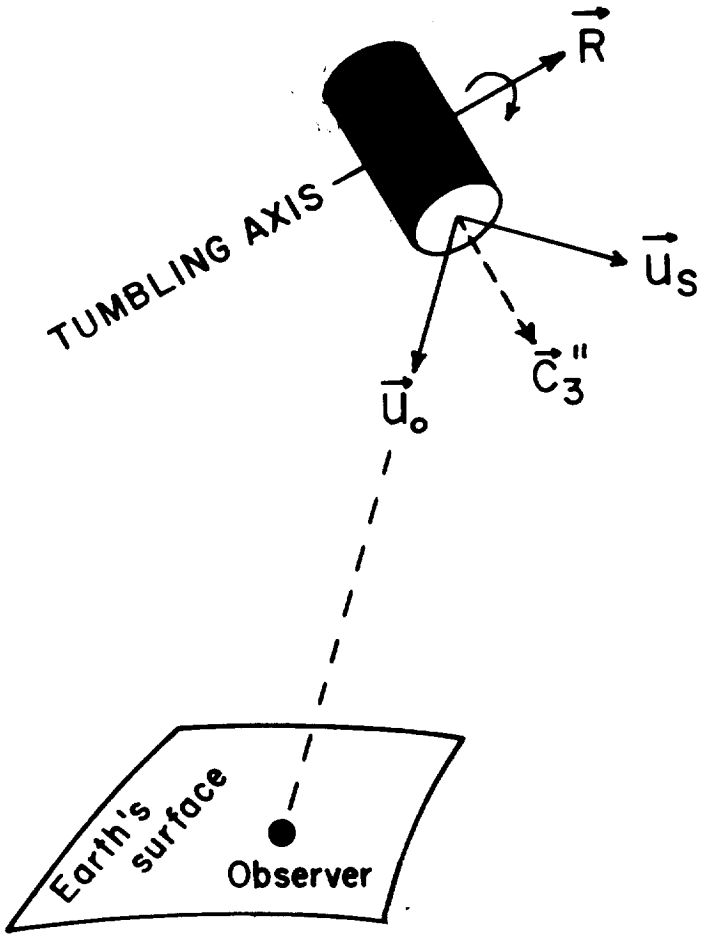

Figure 4.--Tumbling satellite with reflecting plane end

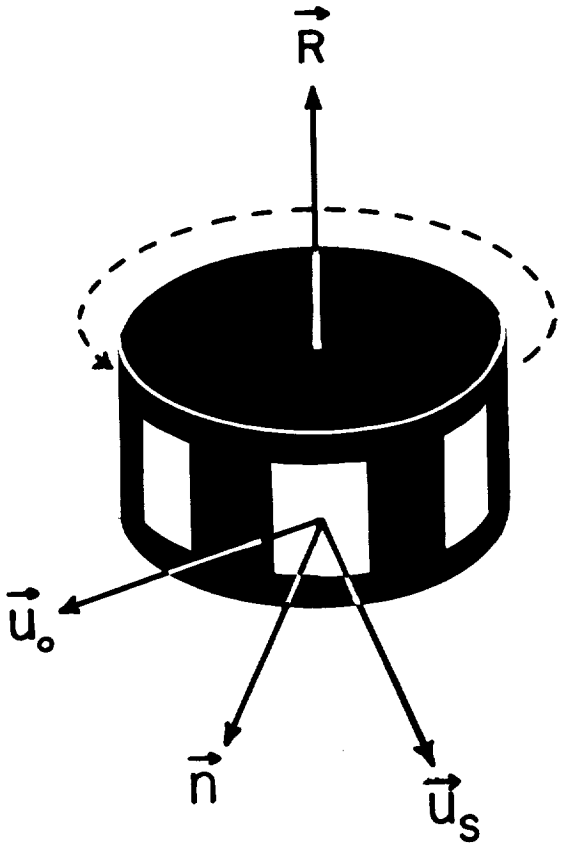

Figure 5.--Spinning satellite with discrete mirrors at the side, (Equivalent to spinning polygonal cylinder.)

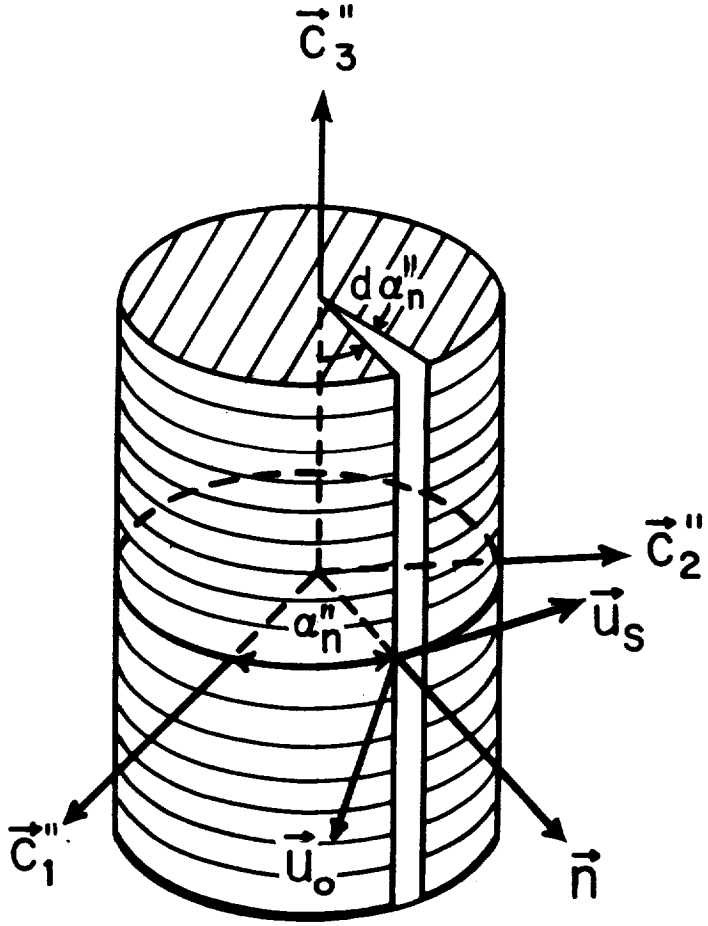

Figure 6.--Body-fixed coordinate system of a cylinder with reflecting side. $\vec{n}$ normal vector on reflecting element of the surface.

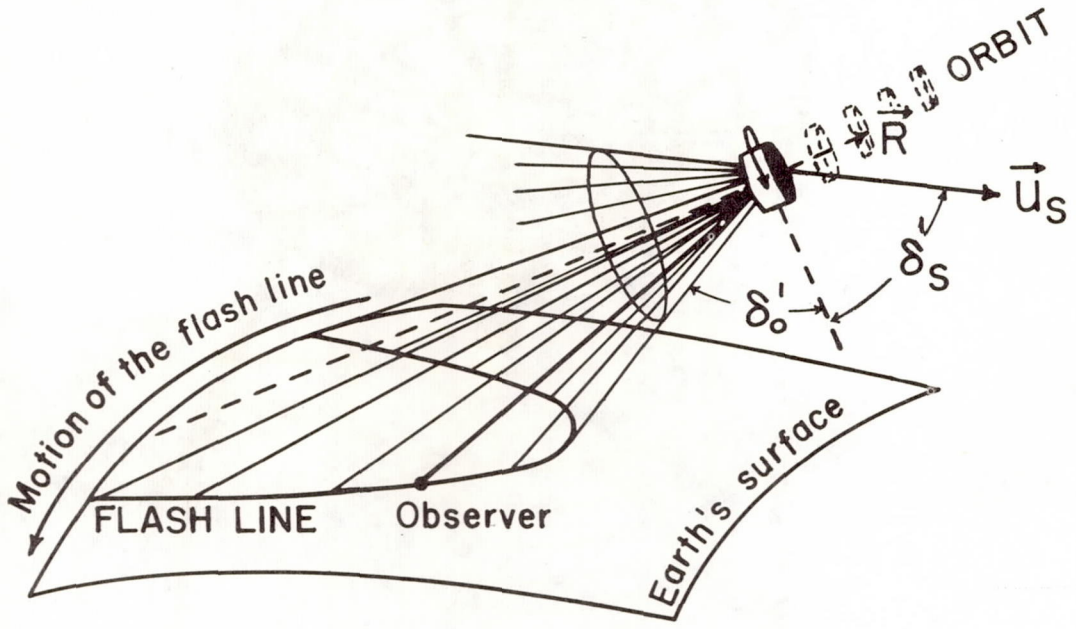

Figure 7.--Geometry of the cone of light as specular-reflected by the side of a spinning cylinder.

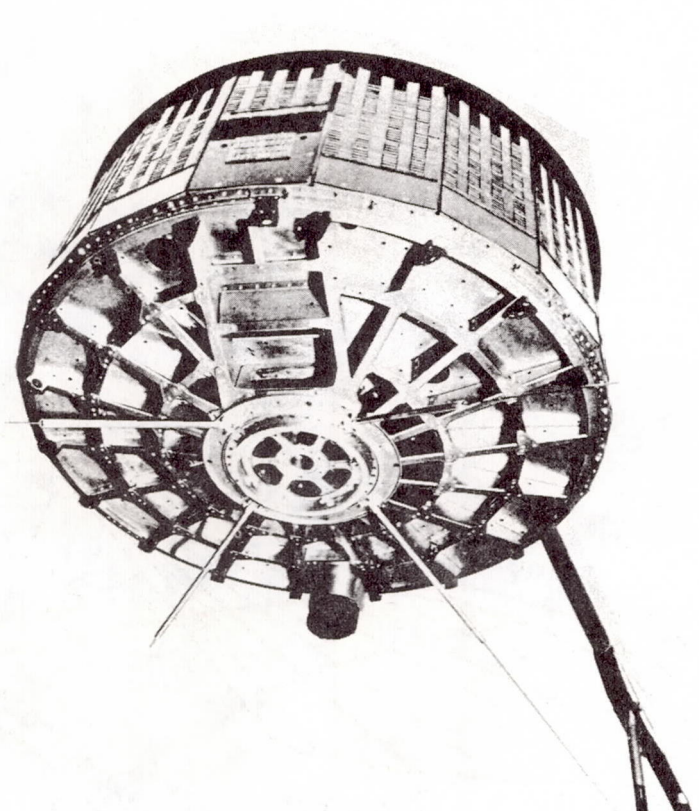

Figure 8.--Tiros II Meteorological Satellite (from NASA Tech. Note D-1293: Telemetering infrared data from the Tiros meteorological satellites, J. F. Davis, R. A. Hanel, R. A. Stampfl, M. G. Strange, and M. R. Townsend)

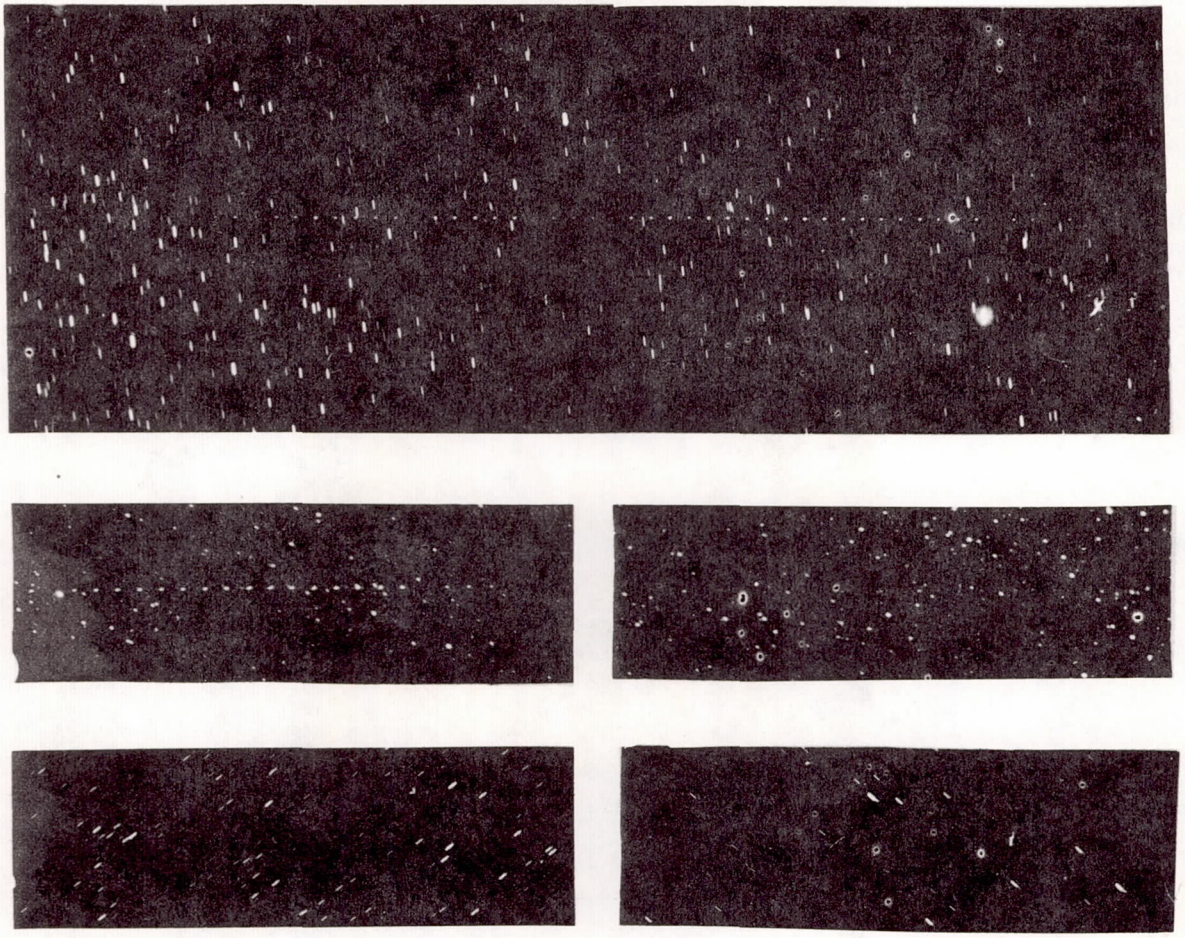

Figure 9.--Trails of satellites on Baker-Nunn stationary exposures

a. 1960 β2 (Tiros I) 1960, July 24, $01^h\ 22^m\ 12^s$ UT
b. 1960 β2 1960, June 2, $23^h\ 29^m\ 03^s$ UT
c. 1960 β2 1960, June 2, $23^h\ 29^m\ 18^s$ UT
d. 1960 ι2 1960, October 16, $08^h\ 38^m$ UT
e. 1960 ι2 1962, April 30, $08^h\ 55^m$ UT

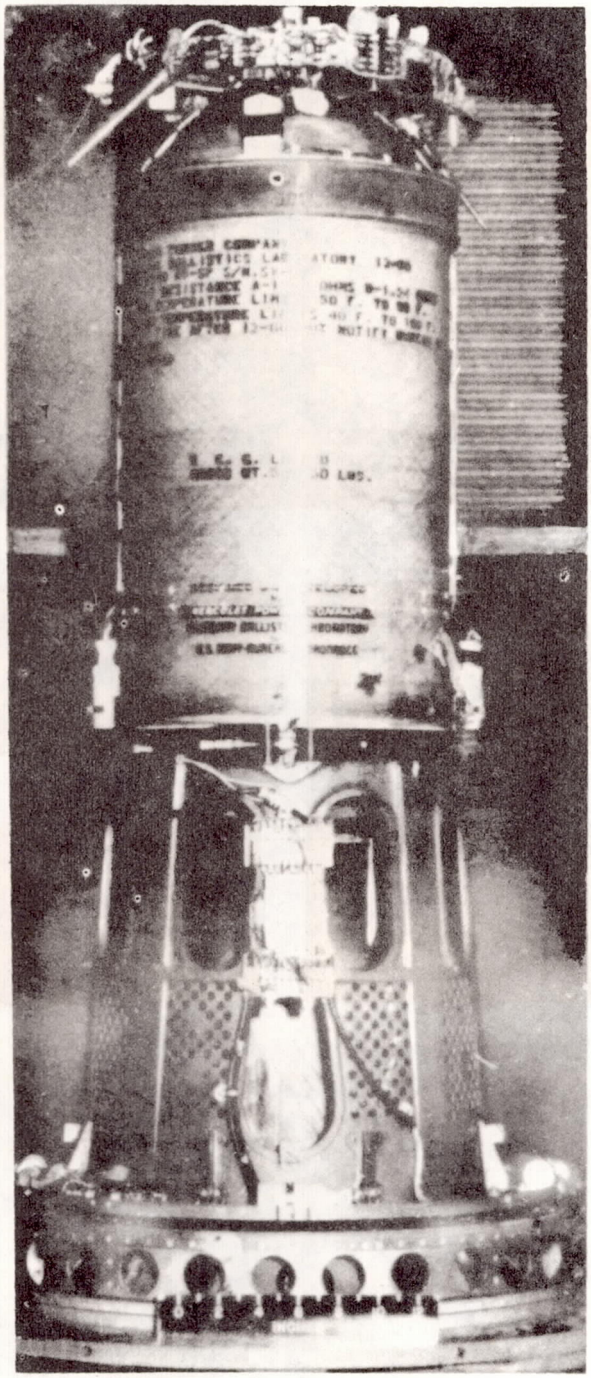

Figure 10.--Carrier Rocket (1960 ι2) of Echo I
(figure from NASA Wallops Station Handbook Vol. II)

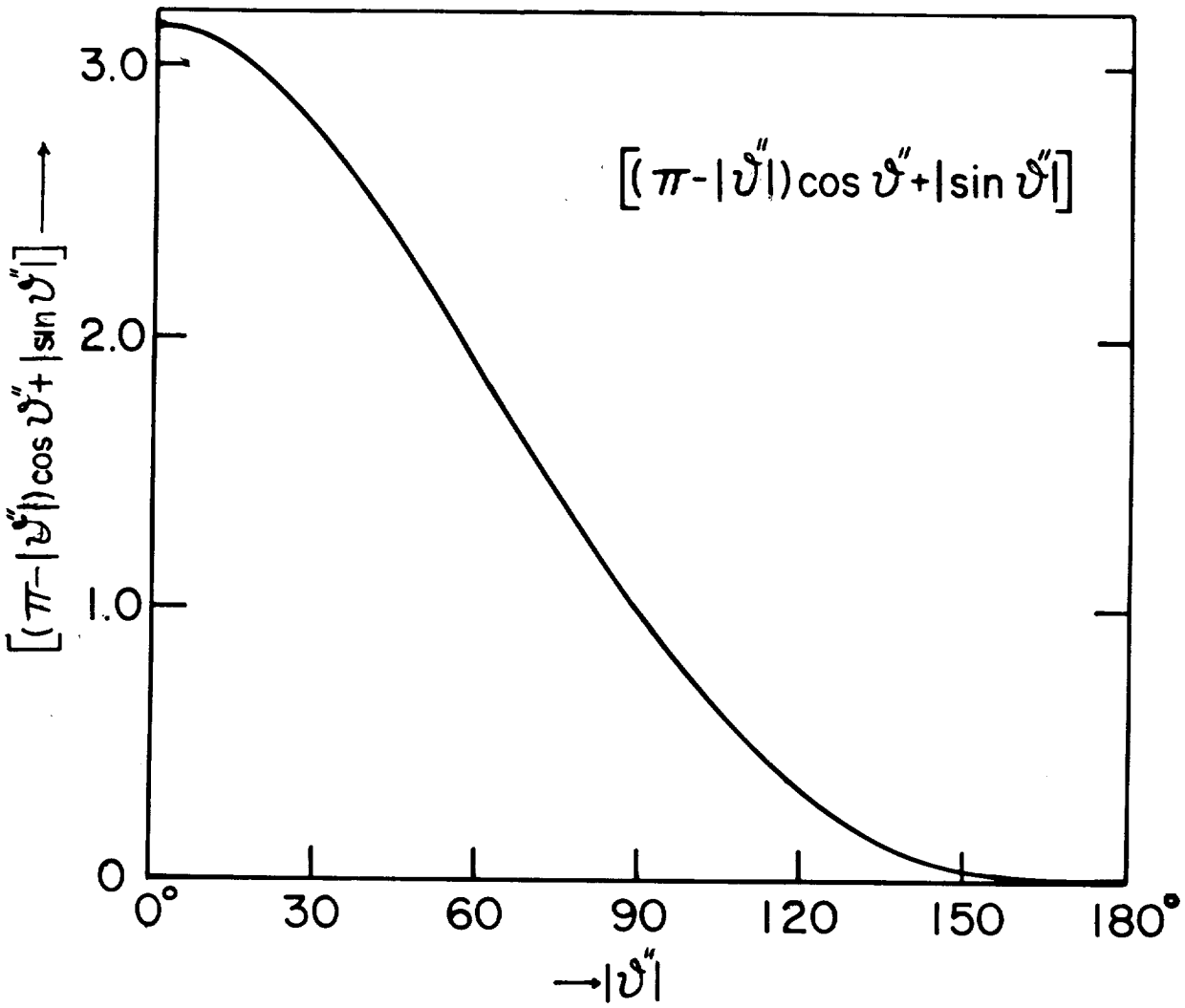

Figure 11.--Dependence of diffuse reflected light intensity (equation (38)) by a cylinder on the difference ν'' of the direction angles between sun (α''_s) and observer (α''_o) in the body system.

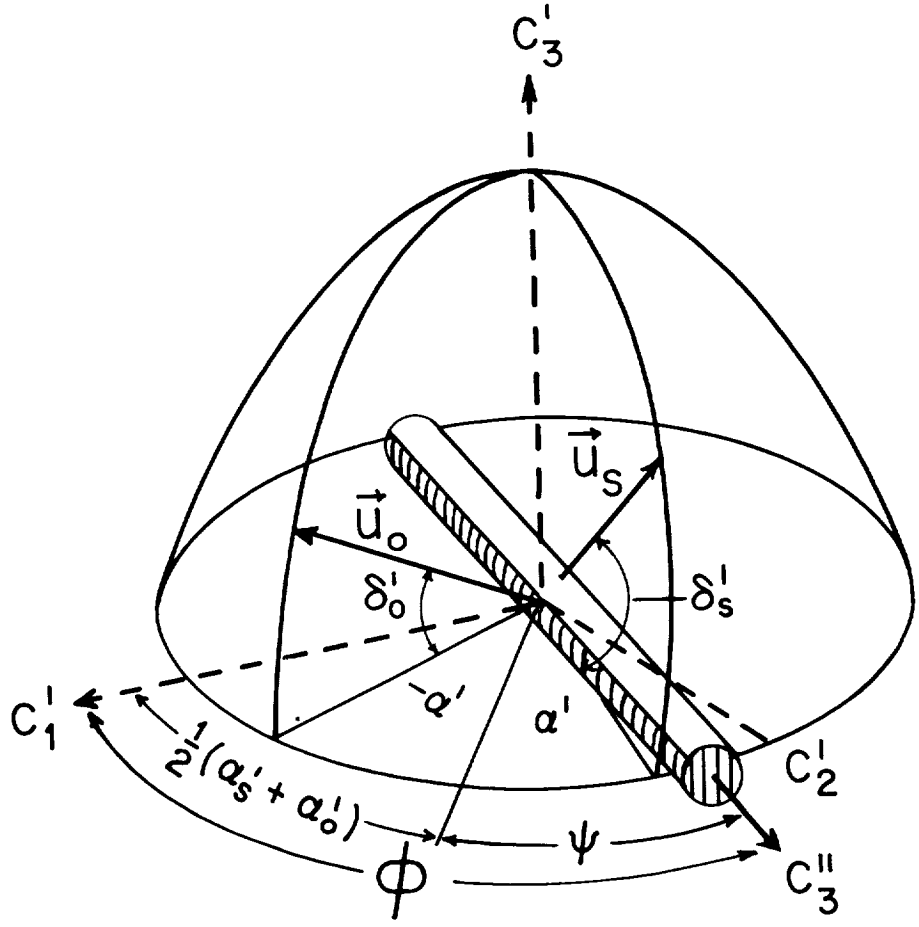

Figure 12.--Tumbling cylinder geometry
Definition of the angles ψ and α'
in the rotational plane system

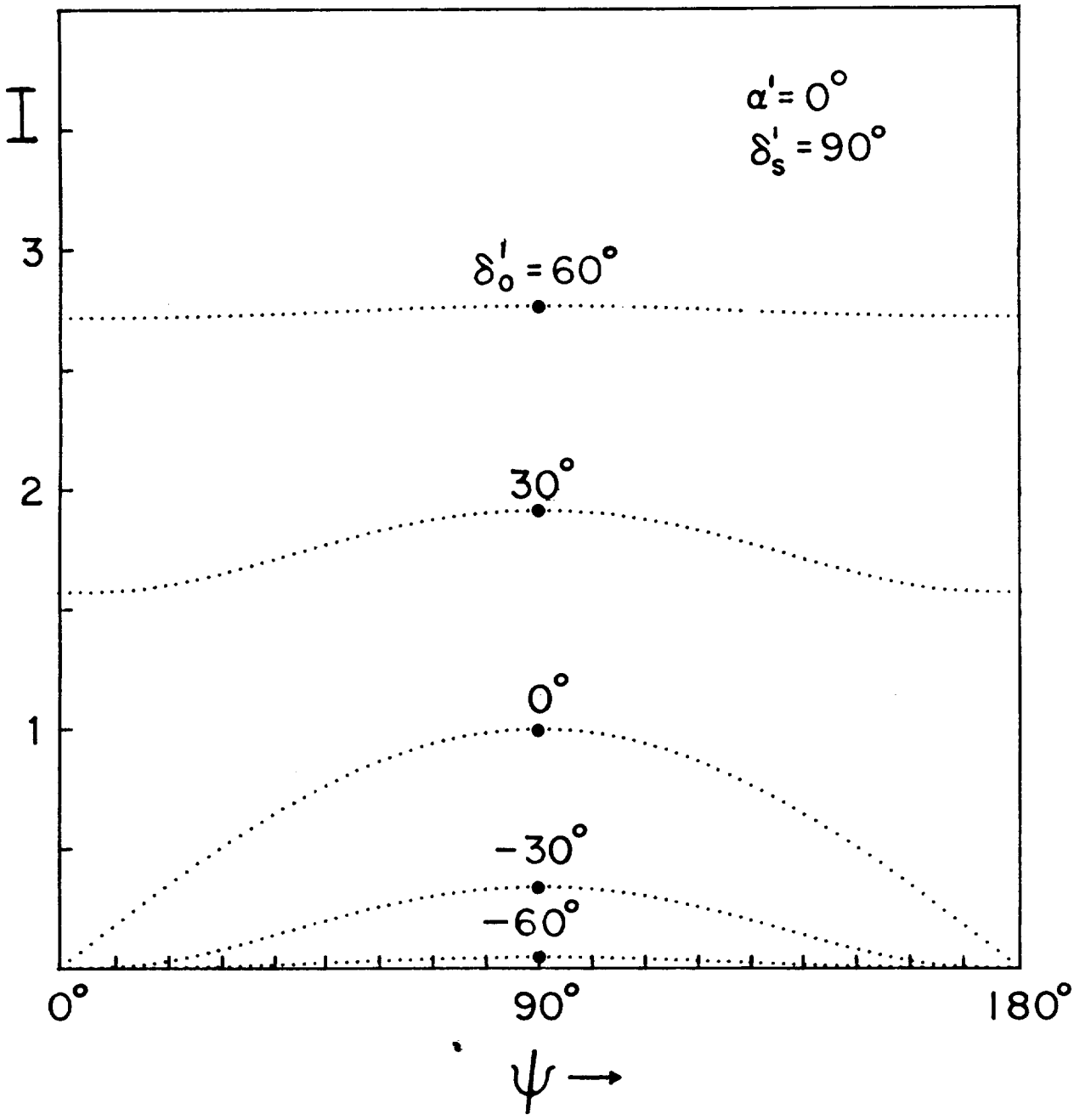

Figure 13

Figures 13 through 21.--Intensity from a tumbling, diffuse reflecting cylinder. Definitions: (see Fig. 12)

α', δ'_s, δ'_o, direction angles of sun and observer

ψ, position angle of the cylinder axis

$\frac{d}{\ell}$, ratio $\frac{\text{diameter}}{\text{length}}$, given for cylinders with reflective ends

I, relative intensity ($J = \frac{F\rho\ell d}{4\pi} \cdot I$)

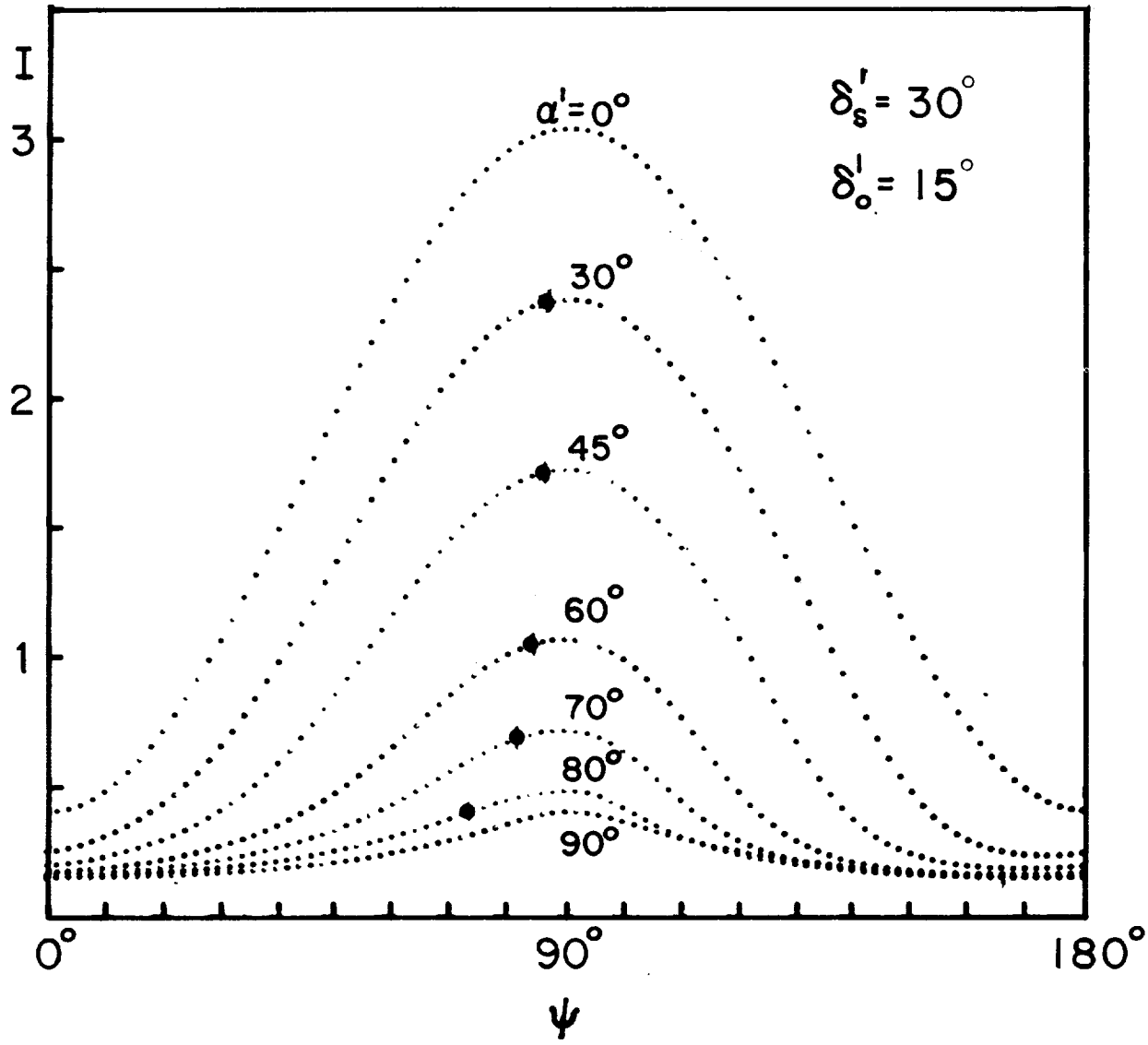

Figure 14

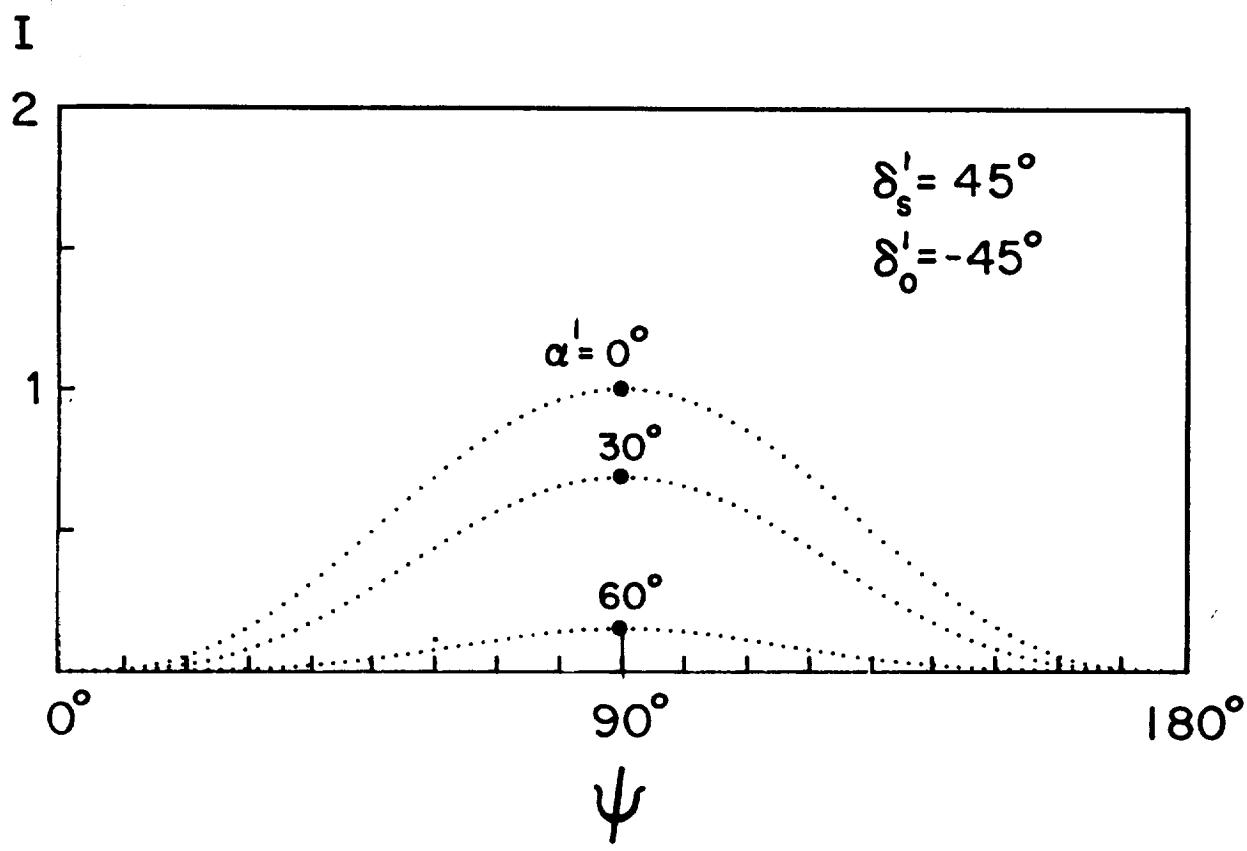

Figure 15

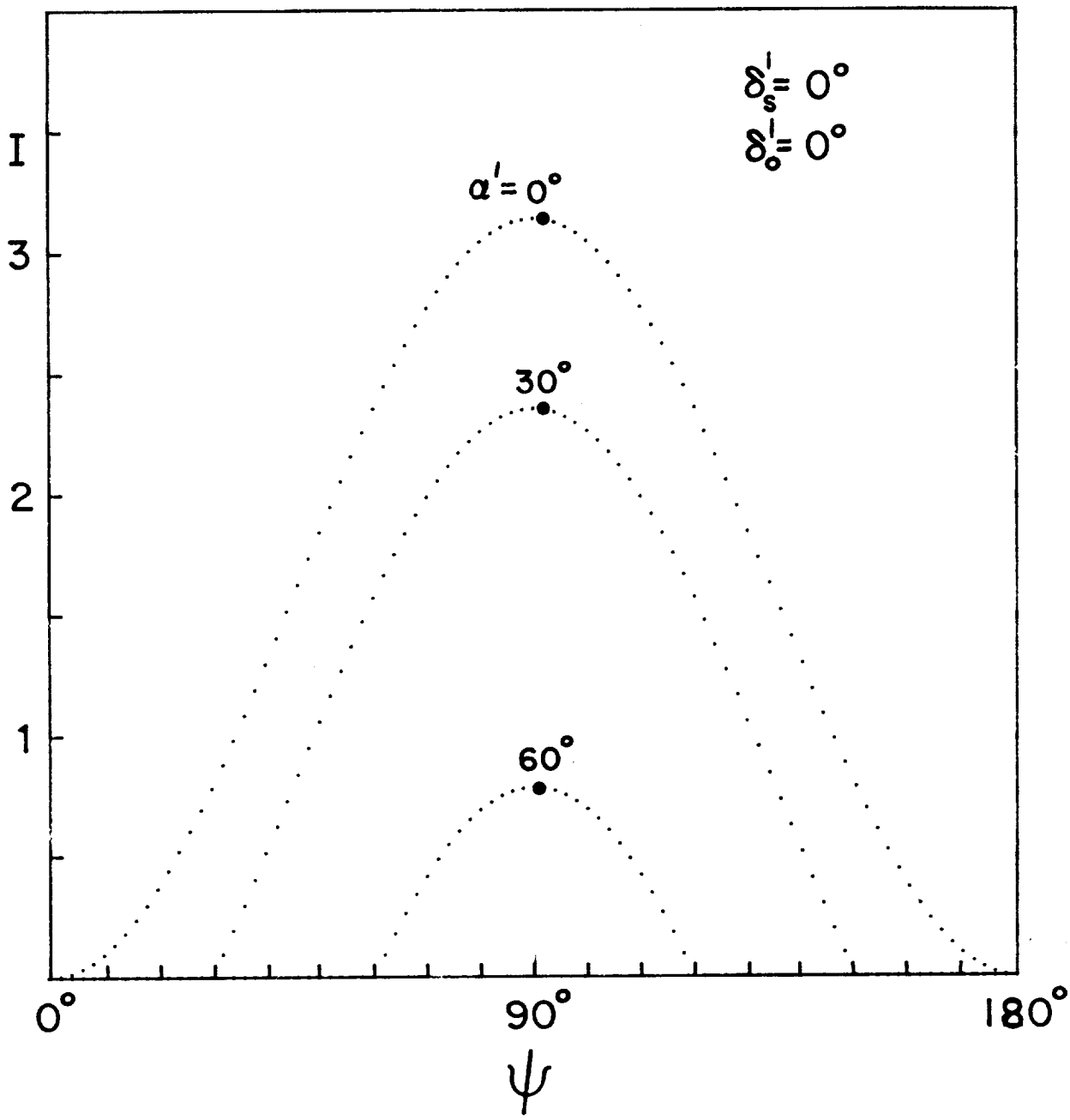

Figure 16

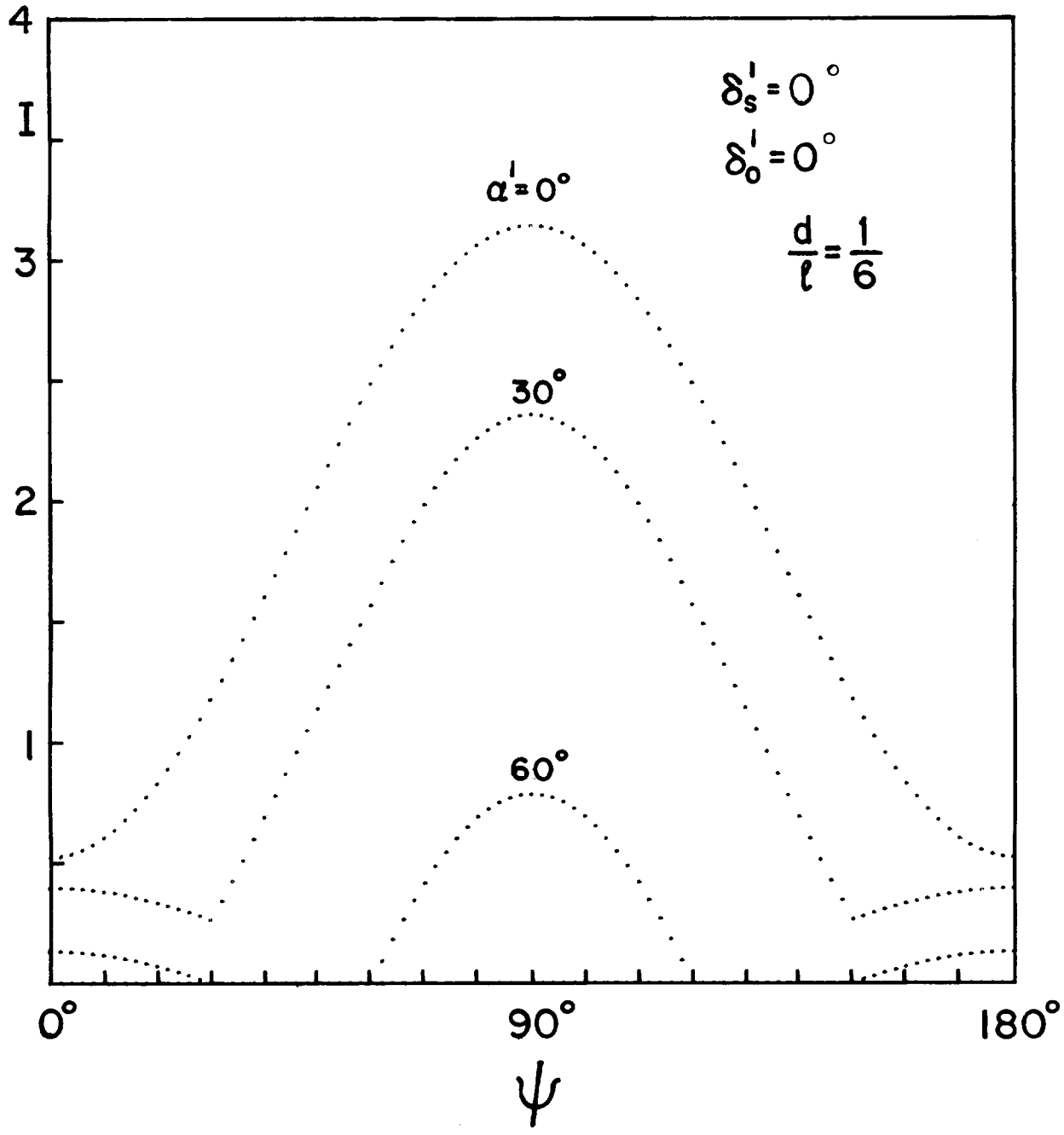
4
I
3
2
1
$\delta_s' = 0°$
$\delta_0' = 0°$
$\alpha' = 0°$
$\frac{d}{\ell} = \frac{1}{6}$
30°
60°
0°
90°
180°
ψ

Figure 17

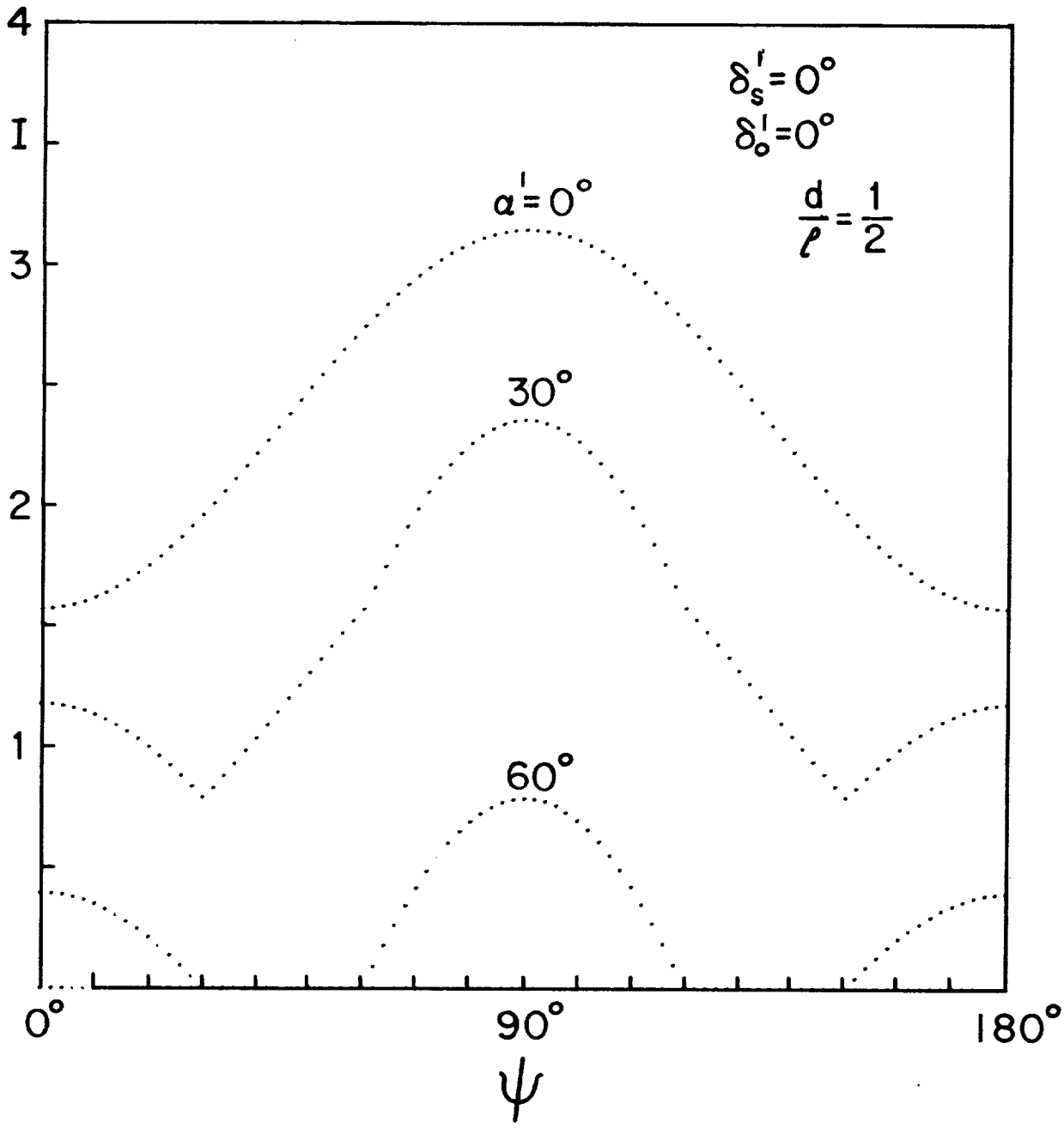
4
I
3
2
1
$\delta_s' = 0°$
$\delta_o' = 0°$
$\alpha' = 0°$
$\frac{d}{\ell} = \frac{1}{2}$
30°
60°
0°
90°
180°
ψ

Figure 18

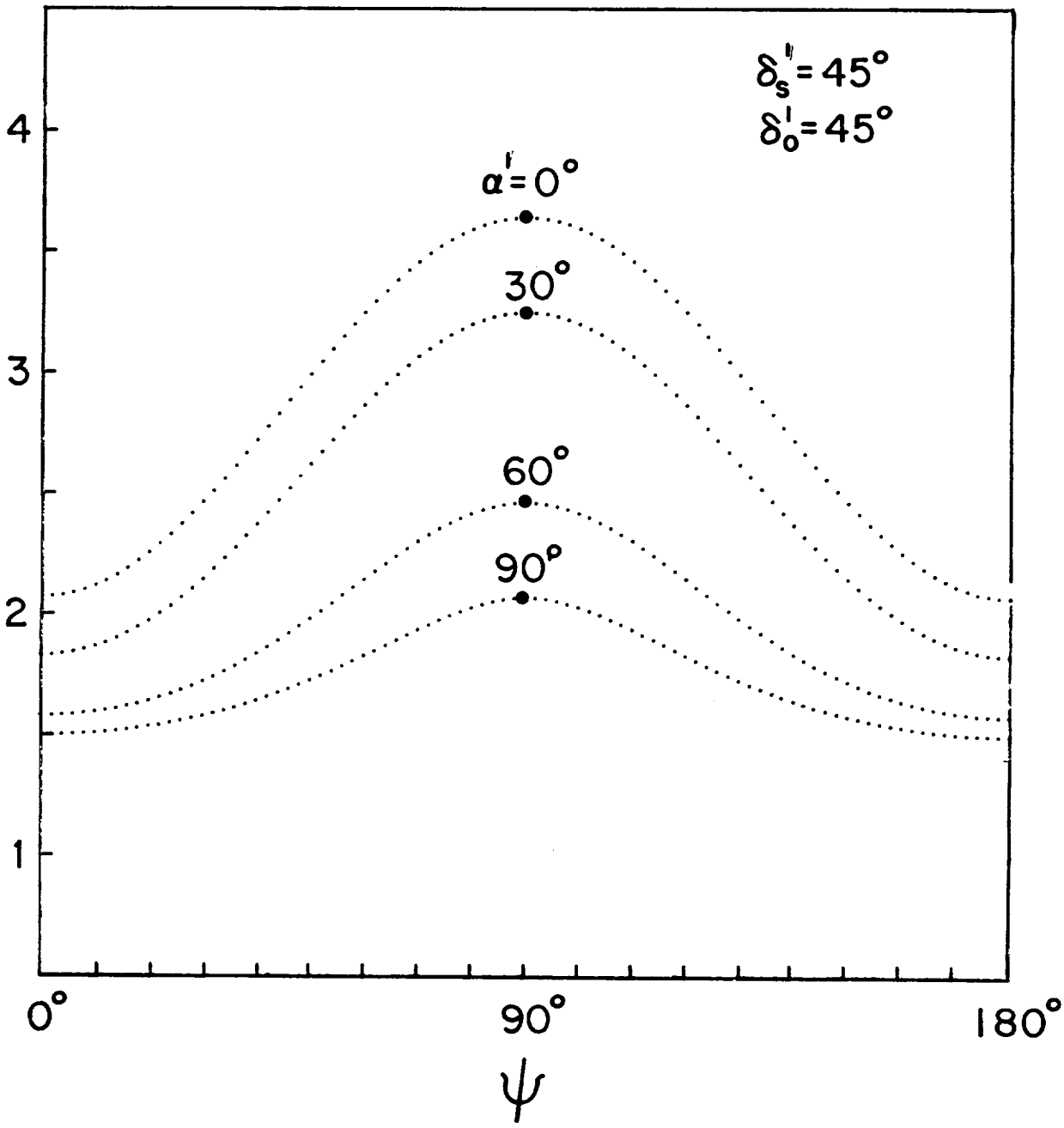

Figure 19

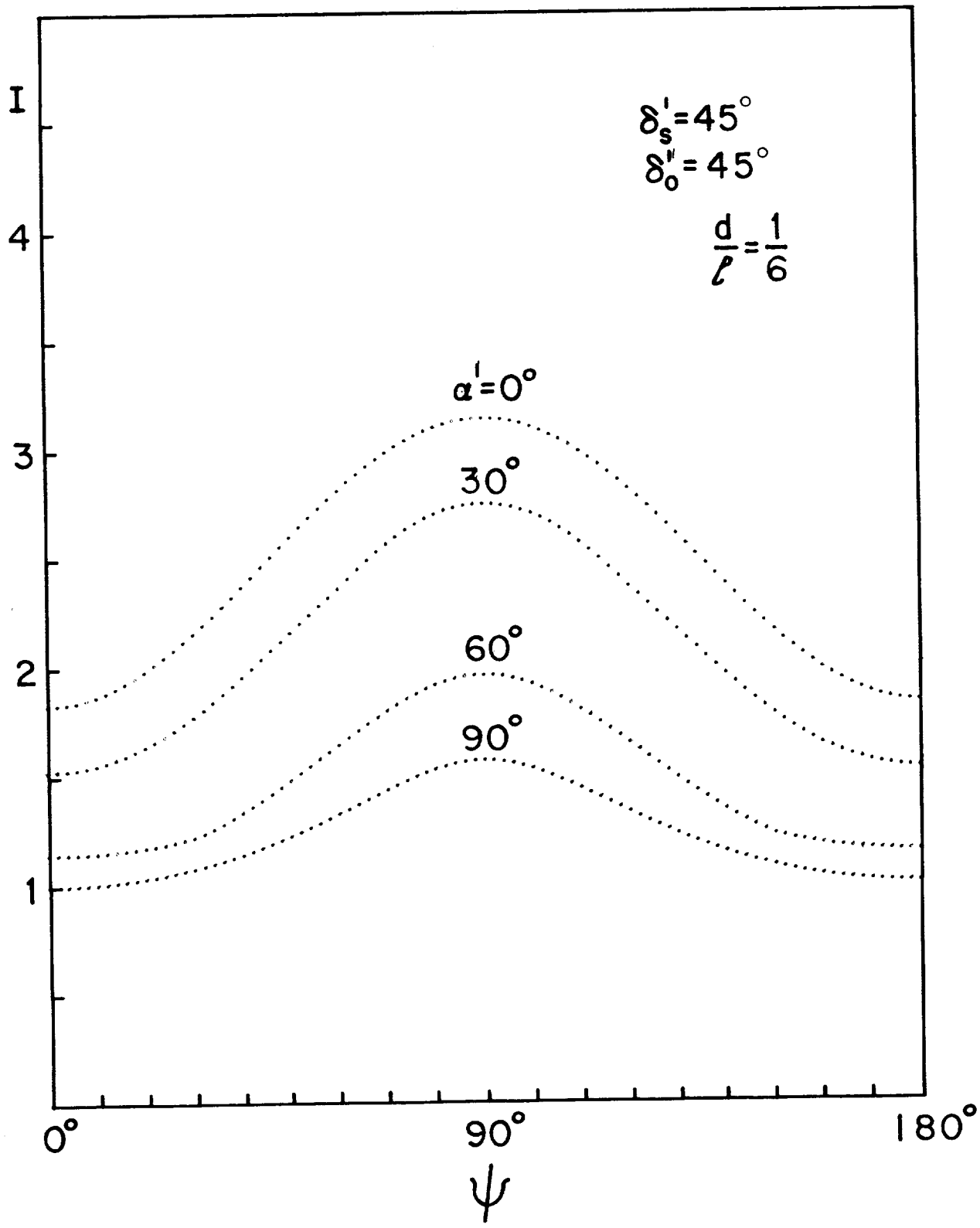
I
4
3
2
1
$\delta_s' = 45°$
$\delta_0'' = 45°$
$\frac{d}{\ell} = \frac{1}{6}$
$\alpha' = 0°$
30°
60°
90°
0°
90°
180°
ψ

Figure 20

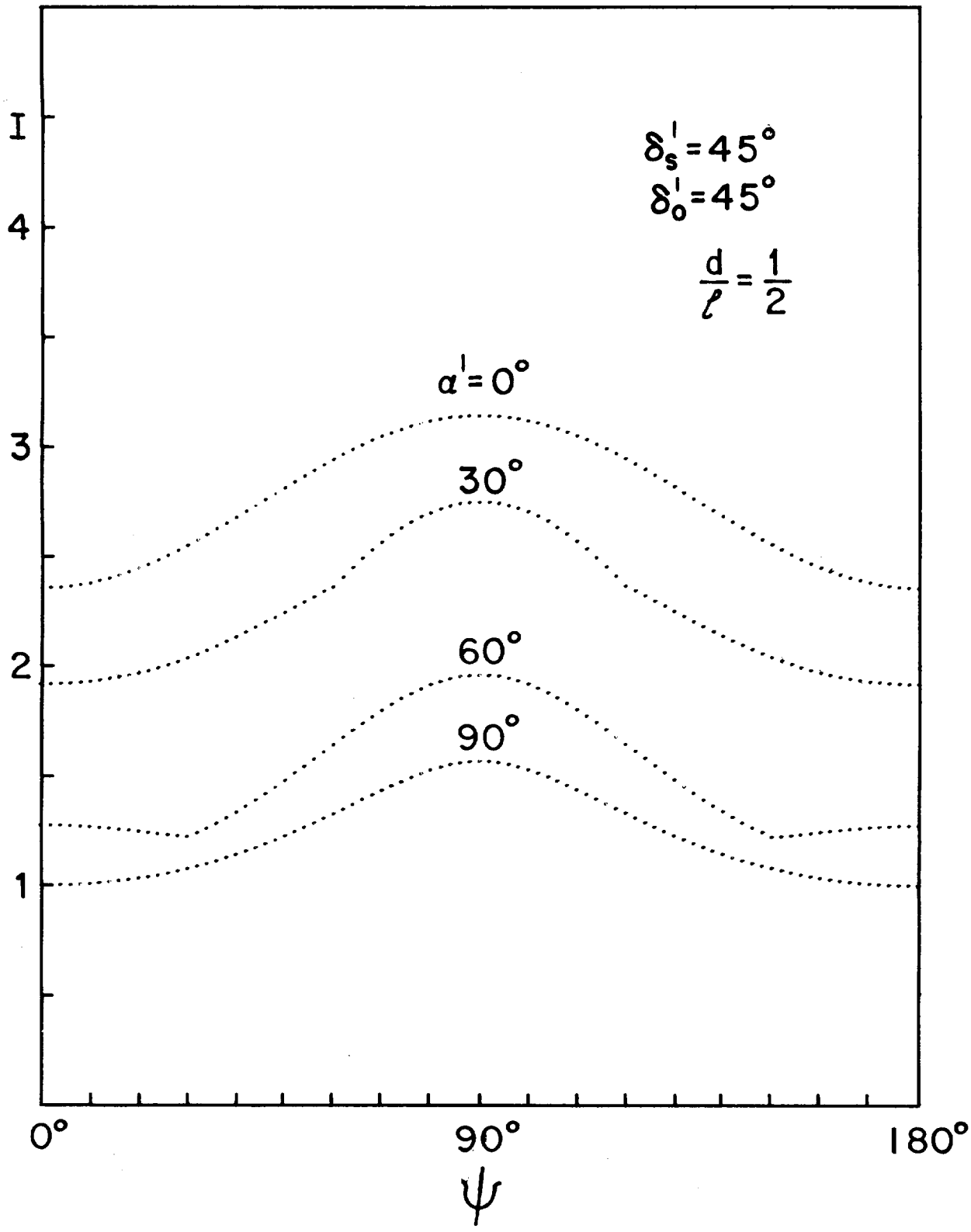
I
4
3
2
1
$\delta_s' = 45°$
$\delta_o' = 45°$
$\frac{d}{\ell} = \frac{1}{2}$
$\alpha' = 0°$
30°
60°
90°
0°
90°
180°
ψ

Figure 21

NOTICE

This series of Special Reports was instituted under the supervision of Dr. F. L. Whipple, Director of the Astrophysical Observatory of the Smithsonian Institution, shortly after the launching of the first artificial earth satellite on October 4, 1957. Contributions come from the Staff of the Observatory. First issued to ensure the immediate dissemination of data for satellite tracking, the Reports have continued to provide a rapid distribution of catalogues of satellite observations, orbital information, and preliminary results of data analyses prior to formal publication in the appropriate journals.

Edited and produced under the supervision of Mr. E. N. Hayes, the Reports are indexed by the Science and Technology Division of the Library of Congress, and are regularly distributed to all institutions participating in the U.S. space research program and to individual scientists who request them from the Administrative Officer, Technical Information, Smithsonian Astrophysical Observatory, Cambridge 38, Massachusetts.